Enhancing Capture Effect over LEO Satellite Within the Framework of Contention Resolution ALOHA

Zhicheng Qu[1,2], Gengxin Zhang[1,2(✉)], Haotong Cao[1,2], and Jidong Xie[1,2]

[1] College of Telecommunications and Information Engineering, NUPT, Nanjing, China
{1015010132,zgx,1015010309,feng}@njupt.edu.cn
[2] TNNERC, NUPT, Nanjing, China

Abstract. Contention resolution diversity slotted ALOHA (CRDSA) with packet repetition and iterative interference cancellation (IIC) has been proven that achieves 48% improvement in terms of throughput than pure slotted ALOHA which merely has a theoretical throughput upper bound of 0.36. So far, optimizations of such random access scheme have been proposed in the literature called irregular repetition slotted ALOHA (IRSA) and coded slotted ALOHA (CSA) which both targeted the collision channel model. In this paper, the environment of LEO satellite communication and capture effect at the satellite receiver are considered. Meanwhile, due to the inherent propagation feature of LEO satellite, capture effect can be enhanced through separating LEO footprint into districts. Under a setting of finite frame length, this separating scheme is analyzed via Monte Carlo simulation combining with optimized power control. Numerical results are provided, which prove the stability of proposed scheme when channel load exceeding 1.

Keywords: Capture effect · Internet of things · LEO satellite · Power diversity · Random access

1 Introduction

Satellite communication, especially for LEO satellite, has a growing capability for numerous kinds of applications including internet access, supervisory control and data acquisition (SCADA), and internet of things (IoT) [1]. Under this background, a high efficient medium access control (MAC) scheme is needed for ensuring communication quality. Random access (RA) schemes, as their nature of avoiding signalling overhead and providing short transmission latencies, have become a candidate for MAC in satellite communication.

Initiating with the ALOHA scheme proposed by Abramson [2] in 1970, which has a maximum expected throughput of 0.18, various evolutional RA protocols

Supported by National Science Foundation of China under Grant No. 91738201 and No. 61801445.

M. Jia et al. (Eds.): WiSATS 2019, LNICST 281, pp. 552–561, 2019.
https://doi.org/10.1007/978-3-030-19156-6_52

have been published in literature. Slotted ALOHA (SA) [3] introduced the concept of frame and slot into pure ALOHA, and the theoretical maximum throughput of SA has reached 0.36. Furthermore, an improvement of SA called diversity slotted ALOHA (DSA) [4] with packet repetition has been proposed. Under the condition of light traffic load, DSA has performance improvement in transmission delays w.r.t. SA. Contention resolution ALOHA (CRA), an epoch-making enhanced kind of DSA beginning with contention resolution diversity slotted ALOHA (CRDSA) [5], has been proposed with two novel approaches: (1) each packet replica has a pointer directing to the other replicas; (2) receiver uses iterative interference cancellation (IIC). Liva adopted the knowledge of bipartite graphs to describe the transmitting and IIC process of CRDSA. Meanwhile, in [6], the author proposed a novel scheme with irregular packet repetition degree (i.e., each packet may choose different numbers of replicas under a chosen distribution) called irregular repetition slotted ALOHA (IRSA), which can achieve maximum throughput of 0.97 for large frames whereas for CRDSA the value is 0.55. Additionally, a ALOHA-based scheme with the combination of packet erasure correcting codes and IIC called coded slotted ALOHA (CSA) [7] can asymptotically reach the ultimate throughput for collision channel model.

Collision channel model, however, is far from the practical channel situation due to the assumption that no transmission suffered from colliding can be recovered. In common fading channel model, capture effect [8] caused by fading-oriented power variations ensures successful decoding of the sufficiently strong signal even under colliding. Apparently, the LEO satellite channel suffers from fading and shadowing, and the channel state dramatically varies with the elevation angle. In [9], the modeling of LEO satellite channel and the method for analyzing capture probability using SA scheme was presented.

In this paper, we extend the analysis of capture effect in LEO satellite channel within the CRA framework. First, within the capture model of threshold, we derive the expression of capture probability over LEO satellite channel. Next, we intend to enhance the inherent capture effect of LEO satellite system by separating the footprint into districts according to elevation angle α. Among those districts, an optimized power control mechanism is proposed in order to increase the power differential at receiver as well as the capture probability. Finally, the mechanism is investigated within finite frame length via simulations. It is shown that the proposed mechanism indeed enhance the inherent capture effect of LEO satellite communication, and optimize the system performance of throughput.

The paper is organized as follows. Section 2 introduces the system model. Section 3 focuses on expression of capture probabilities for LEO satellite channel. Section 4 presents a ring separating scheme combining with optimized power control among different rings. Section 5 shows the numerical results. Section 6 concludes the paper.

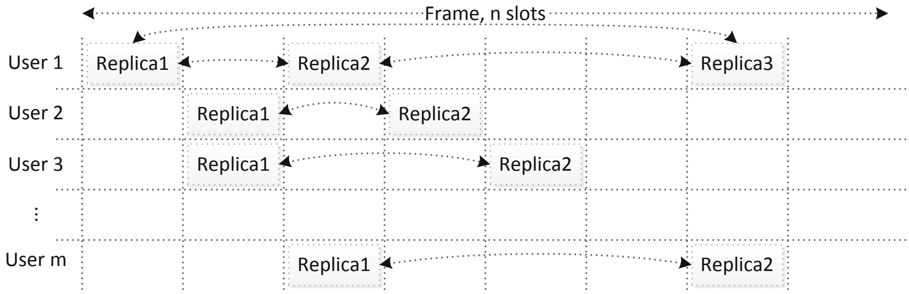

Fig. 1. CRDSA/IRSA scheme.

2 System Model

2.1 Access Protocol and Graph-Based Presentation

On brief overview, the MAC frames have duration of T_f that contain n slots with duration of $T_s = T_f/n$, and each packet transmission can only last for one slot. The normalized channel traffic load G is defined as

$$G = \frac{m}{n} \tag{1}$$

where m is a finite number of users transmitting in a chosen frame. Channel throughput T is a function of G and packet loss rate P_L. Within the framework of CRA, each user choose a repetition degree d independently from a predefined probability mass function (p.m.f) $\{\Lambda_d\}$ and randomly picks up d slots in a frame to transmit d replicas. CRDSA, however, is a special case of CRA that each user has the same repetition degree, which means $\Lambda_d = 1$ for the predefined degree d. Additionally, it is assumed that each replica of the same user contains the whole locating information of the other d-1 replicas. The diagram of CRA protocol is shown in Fig. 1. In [6], the author introduced a bipartite graph-based presentation of CRA scheme. As depicted in Fig. 2, a bipartite graph $\mathcal{G} = \{U, S, E\}$ can fully represent a MAC frame of CRA. $\mathcal{G}$ contains a set U of m user nodes, and a set S of n slot nodes in a frame, and a set E of edges representing each transmitted replica. An edge connects an user node $u_k \in B$ with a slot node $s_j \in S$ iif user k transmits a replica in slot j. Meanwhile, the IIC process of CRA is also presented in Fig. 2. The dashed edge represents a replica transmitted in a collision-free slot so that the other edge connected with the same user node can be removed. After one iteration, the receiver will find another collision-free slot node and repeat the IIC process until meeting the end condition.

The concept of *node-* and *edge-perspective degree distribution* is useful for further analysis. Polynomial representation of user-node and slot-node degree distribution are $\Lambda(x) = \sum_{d=2}^{d_{\max}} \Lambda_d x^d$ and $\Psi(x) = \sum_{c=0}^{m} \Psi_c x^c$, respectively. Λ_d (Ψ_c) denotes the probability that an user node (slot node) possessing d (c)

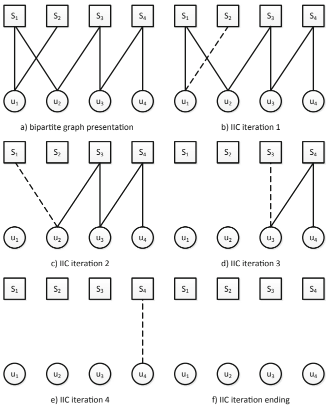

Fig. 2. Bipartite graph-based presentation of CRA.

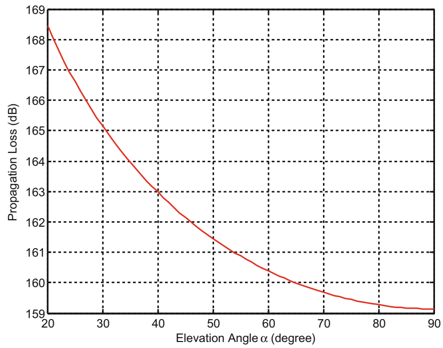

Fig. 3. Free space loss corresponding to α.

edges. As mentioned before, $\{\Lambda_d\}$ is fully controlled by the system while Ψ_c is determined by the traffic load G

$$\Psi_c = \binom{m}{c} \left(\frac{G/R}{m}\right)^c \left(1 - \frac{G/R}{m}\right)^{m-c} \tag{2}$$

where R is the scheme rate defined as the inverse of average repetition degree

$$R = \frac{1}{\bar{\bar{d}}} = \frac{1}{\sum_{d=2}^{d_{\max}} d\Lambda_d}. \tag{3}$$

Similarly, edge-perspective degree distribution can be defined as the p.m.f $\{\lambda_d\}_{d=2}^{d_{\max}}$ and $\{\psi_c\}_{c=0}^{m}$. λ_d is the probability that an edge is linked to a *d-degree* user node, and likewise ψ_c is the probability that an edge is linked to a *c-degree* slot node. Easily, the corresponding polynomial representation of the two distributions are $\lambda(x) = \sum_{d=2}^{d_{\max}} \lambda_d x^{d-1}$ and $\psi(x) = \sum_{c=0}^{m} \psi_c x^{c-1}$. Note that $\lambda(x) = \Lambda'(x)/\Lambda'(1)$ and $\psi(x) = \Psi'(x)/\Psi'(1)$.

2.2 LEO Channel Model

Free space loss is considered as the most important attenuation in LEO channel, and it is calculated as

$$L_{FS} = 32.45 + 20\lg(D) + 20\lg(f) \tag{4}$$

where D is the link distance in kilometers and f is the operating frequency in Mega Hertz. Assuming the LEO orbit altitude is 900 km and operating frequency is 2400 MHz, the free space loss corresponding to α is depicted in Fig. 3.

Table 1. Coefficient values for empirical formulas at different elevation angles

α	K	μ	σ
20°	1.6929	−0.73508	3.5
40°	2.8734	−0.16524	2.5
60°	6.2734	−0.09636	1.5
80°	11.8926	−0.00332	0.5

In [10], the authors proposed a statistical model of LEO satellite channel. In this model, the distribution of received signal envelop is a combination of Ricean and lognormal distribution, which has the probability density function (p.d.f) of

$$f_P(p) = \int_0^\infty f(p|S)\, f_S(S)\, dS \tag{5}$$

where $f(p|S)$ is a Rice p.d.f under a certain shadowing S

$$\begin{aligned} f(p|S) = 2(K+1)\frac{p}{S^2}\exp\left(-(K+1)\frac{p^2}{S^2} - K\right) \\ \cdot I_0\left(2\frac{p}{S}\sqrt{K(K+1)}\right) \end{aligned} \tag{6}$$

and $f_S(S)$ is a lognormal distribution that S follows

$$f_S(S) = \frac{1}{\sqrt{2\pi}\sigma S}\exp\left(-\frac{1}{2}\left(\frac{\ln S - \mu}{\sigma}\right)^2\right). \tag{7}$$

In (5) and (6), $I_0(\cdot)$ is the zero order modified Bessel function, K is the Rice factor, μ and σ are the mean and the variance of the associated normal variate, respectively. To be noticed, K, μ and σ are associated with α between 20° and 80° degree through empirical formulas

$$\begin{aligned} K(\alpha) &= K_0 + K_1\alpha + K_2\alpha^2 \\ \mu(\alpha) &= \mu_0 + \mu_1\alpha + \mu_2\alpha^2 + \mu_3\alpha^3 \\ \sigma(\alpha) &= \sigma_0 + \sigma_1\alpha \end{aligned} \tag{8}$$

and the empirical value of the three coefficients are listed in Table 1.

3 Capture Probabilities

In this framework, the receiver can discriminate between empty slots and busy slots. The probability that replica i in slot j is successfully recovered is called capture probability. Under threshold-based capture model, signal to interference and noise ratio SINR is the determining factor of capture probability. When the

SINR of replica i exceeds a certain threshold r_{th}, it is considered to be captured, i.e.,

$$\Pr\{\text{replica } i \text{ is caputured}\} = \begin{cases} 1, & SINR_i \geqslant r_{th} \\ 0, & \text{otherwise} \end{cases} \tag{9}$$

In (8), $SINR_i$ is defined as follows

$$SINR_i = \frac{P_{ij}}{N + \sum_{m \neq i} P_{mj}} \tag{10}$$

where P_{ij} is the receiving power of i-th packet, and $\sum_{m \neq i} P_{mj}$ denotes the total power of rest packets in slot j.

On graph viewing, at a specific time during the decoding process of a MAC frame, a slot node j may have a node degree of d. To be noticed, after perfect inter-slot and intra-slot (capture) SIC, d is not greater than the original node degree of d_j. Now, we randomly choose one packet from the d packets and call it the reference packet (RP). Meanwhile, the probability that RP is successfully recovered merely through intra-slot SIC is denoted as $C(d,t)$, where $1 \leq t \leq r$ is the iteration step after the beginning of decoding and in any step prior to t RP cannot be recovered. The total probability $C(d)$ of successfully recovering RP is

$$C(d) = \sum_{t=1}^{d} C(d,t) \tag{11}$$

During intra-slot SIC process, all packets are categorized into two groups in the rule of power. Packets in the first group with stronger power than RP are arranged in a descending order by their powers (i.e., $P_1 \geqslant P_2 \geqslant \cdots \geqslant P_{t-1}$), and the rest packets in the second group are not arranged. Under such arrangement, the probability that at least t packets successfully recovered is denoted by

$$\rho(t) = \Pr\{SINR_1 \geqslant r_{th}, \cdots, SINR_t \geqslant r_{th}\}$$

and $\rho(t)$ is calculated as follows

$$\begin{aligned} \rho(t) = & \int_0^{\infty} dp_r \cdots \int_0^{\infty} dp_{t+1} \times \int_{r_{th}\left(N+\sum_{i=t+1}^{r} p_i\right)}^{\infty} dp_t \\ & \times \cdots \times \int_{r_{th}\left(N+\sum_{i=2}^{r} p_i\right)}^{\infty} dp_1 f_P(p_r) \cdots f_P(p_1) \end{aligned} \tag{12}$$

Moreover, there are $\frac{(d-1)!}{(d-t)!}$ arrangements that RP is not in the first group. Therefore, we have

$$C(d,t) = \frac{(d-1)!}{(d-t)!}\rho(t) \tag{13}$$

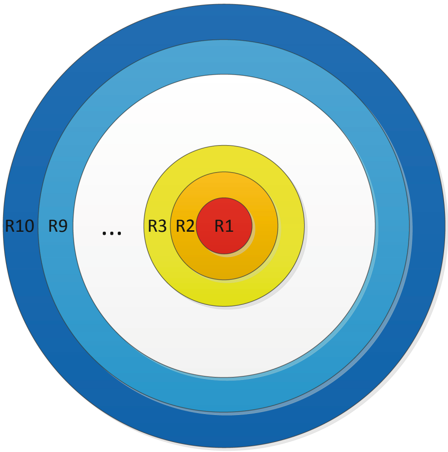

Fig. 4. Ring separating of LEO footprint.

Table 2. Characteristics of each ring

Ring index	Minimum α	Corresponding propagation loss (dB)
1	20.3°	168.3341
2	23.6°	167.0903
3	27.4°	165.8801
4	31.7°	164.7281
5	36.7°	163.6105
6	42.7°	162.5124
7	49.7°	161.4924
8	58.0°	160.5707
9	67.7°	159.8143
10	78.5°	159.3152

In [6], an analysis of SIC convergence was proposed. For a degree-r user node, q is the probability that an connecting edge carries no erasure message, and each other $r-1$ edges have been revealed via previous SIC steps with the probability of $1-l$. Obviously, $q=l^{r-1}$. Similarly, in a degree-c slot node, we have $1-l=(1-q)^{c-1}$ or $l=1-(1-q)^{c-1}$. Therefore, the average erasure probability of an edge during the k-th iteration is

$$q_k=\sum_r \lambda_r q_k^{(r)}=\sum_r \lambda_r d l_{k-1}^{r-1} \tag{14}$$

and

$$l_k=\sum_c \psi_c l_k^{(c)} \tag{15}$$

Taking $C(d,t)$ into consideration, $l_k^{(c)}$ can be expressed as

$$l_k^{(c)}=1-\sum_{d=1}^{c} C(d)\binom{c-1}{d-1} q_k^{d-1}(1-q_k)^{c-d} \tag{16}$$

where $\binom{c-1}{d-1} q_k^{d-1}(1-q_k)^{c-d}$ is the probability that the chosen slot node's degree drops to d. Combining with the edge-perspective degree distribution in Sect. 2.1, where $\psi_c=\exp\{-G/R\}(G/R)^{c-1}/(c-1)!$ when $m\to\infty$ and G/R is constant, l_k corresponds to

$$l_k=1-e^{-\frac{G}{R}}\sum_{c=1}^{\infty}\left(\frac{G}{R}\right)^{c-1}\sum_{d=1}^{c}\frac{C(d)}{(d-1)!}q_k^{d-1}(1-q_k)^{c-d} \tag{17}$$

By combining (14) and (16) with the initial value $q_0=1$, a density evolution recursion [11] can be exploited to express the asymptotic performance of proposed scheme. However, since the channel fading and free space loss vary from α, there cannot be a exact expression of $C(d)$ through mathematical analysis. Hence, in Sect. 5, we take advantage of Monte Carlo simulation to provide numerical results of the scheme.

4 Enhancing Capture Effect with Ring Separating and Power Control

As an inherent phenomenon in LEO channel, power imbalance is inevitable at the receiver caused by fading and propagation loss that requests system design of higher link margin to compensate. This flaw, however, can be utilized in raising throughput performance via capture effect demonstrated in Sect. 3. In general, all users within a LEO satellite footprint have the same opportunity to transmit their packets, and the corresponding capture effect is called natural capture effect without any control mechanism. As mentioned before, the essence of capture effect is the power differential of receiving packets, which caused by varying propagation loss and fading corresponding to α. To enhance capture effect, an efficient way is to enlarge power differential by exploiting features of LEO satellite communication.

On the contrary to terrestrial cellular communication, in LEO satellite communication, users' irregular movements are replaced by the deterministic satellite orbit movement, which can be precisely predicted by the users. In order to enlarge power differential at receiver, the whole LEO footprint can be separated into different rings according to the value of elevation angle α. Obviously, for inclining LEO satellite orbit, this separation will lead no priority to any user. As shown in Sect. 2.2, the propagation loss and the mean value of fading are in a descending order as α increasing. Assuming a footprint is separated into M rings, where each ring has a allowable transmitting probability $P_i (1 \leq i \leq M)$. Under the circumstance that $P_i = 0$, user belongs to ring i is closed and forbidden transmitting. To be noticed, natural capture effect is achieved by setting all P_i equally. In order to enhance capture effect, i.e. reaching sufficient power differential, the rings which suffer medium propagation loss and fading will be shut down (i.e, corresponding $P_m = 0$) while rings of the strongest and lowest attenuation remain fully available with corresponding $P_i = 1$ $(i \neq m)$. By changing P_i, system will be adaptive to various kinds of traffic and be more efficient. For further enlarging the receiving power differential, a simple method is to add extra power to the rings that suffer the lowest propagation loss and fading.

5 Numerical Results

For example, Fig. 4. shows that a footprint (with altitude $h = 900\,\text{km}$ and $\alpha \geq 20°$) is equally separated into 10 rings. Meanwhile, the minimum elevation angle and propagation loss of each ring is presented in Table 2. For sufficient power differential (e.g., 6 dB), the allowable transmitting rings will be Ring No.

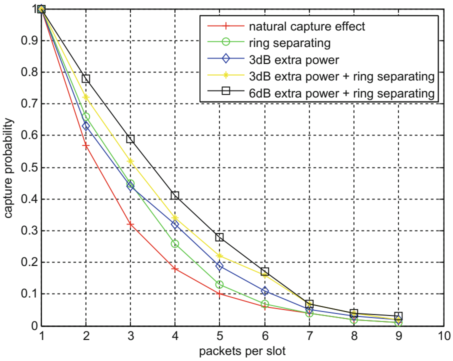

Fig. 5. Capture probability under different schemes.

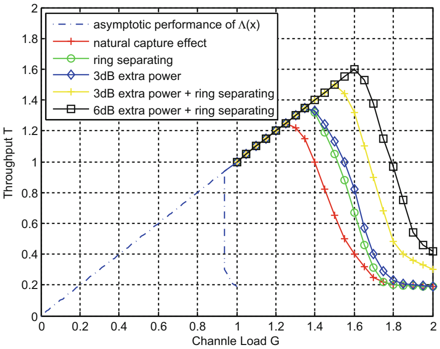

Fig. 6. Throughput performance versus channel load.

1, 2, 9 and 10. We tested the capture probability of the strongest packets and the throughput performance through Monte Carlo simulations under assumption of (1) all users are uniformly distributed in the footprint; (2) capture probability of the strongest packet is (9). Meanwhile, for practical consideration, i.e. limiting the number of pointers in the packet header, the user-node degree distribution is set to $\Lambda(x) = 0.5x^2 + 0.28x^3 + 0.22x^8$, which has a theoretical throughput threshold $G^* = 0.938$ under collision channel model [6]. The other system parameters are set that frame length $n = 200$ slots, $r_{th} = 6$ dB, iteration times $I_{max} = 20$. Figure 5 illustrates the capture probability of the strongest packet. As expected, ring separating scheme raises capture probability of 10% averagely comparing to natural capture. Combining ring separating and extra power compensation (6 dB), the performance is almost 2 times better than natural capture. In Fig. 6, system throughput, defined as the average recovered packets per slot, versus channel traffic load G is provided. The blue dash line is the asymptotic performance of IRSA with the selected user-node degree distribution. By taking capture effect into consideration, all circumstances exhibit peak throughput exceeding 1 [packet/slot], which is the strict upper bound under collision channel. Natural capture can achieve the throughput of 1.26 [packet/slot] while ring separating scheme is able to reach 1.34 [packet/slot] and the stable operating range (i.e., the maximum traffic load that leads to a 20% drop of peak throughput) extend to $G_{sta} = 1.5$, i.e., 60% of gain comparing to the original $G_{sta} = 0.94$. Moreover, within the stable operating range, pure ring separating scheme has a similar performance to that of 3 dB extra power. Similarly, by combining ring separating scheme and extra power compensation (e.g., 3 dB and 6 dB), the peak throughput can reach 1.49 and 1.61 [packet/slot]. Additionally, corresponding gains on stable operating range are 72% and 90%, respectively.

6 Conclusions

The analysis of contention resolution ALOHA over a LEO fading channel, assuming capture effect, is presented in this paper. We provide the expression of capture probability of a reference packet with intra-slot SIC. The closed form approximation, however, is unable to be derived due to LEO channel's fading characteristic, which is a set of PDFs corresponding to α. In addition, we presented a ring separation of LEO footprint combining with power control mechanism in order to enhance capture effect and rasing the system efficiency. Numerical results show that merely taking capture effect into consideration can provide stable performance for channel load values well above 1 [packet/slot]. In a finite frame length with 200 slots, the peak throughput reaches 1.6 [packet/slot] by combining ring separating and power control.

References

1. Qu, Z., Zhang, G., Cao, H., Xie, J.: LEO satellite constellation for internet of things. IEEE Access **5**, 18391–18401 (2017)
2. Abramson, N.: The ALOHA system: another alternative for computer communications. In: 17–19 November 1970, Fall Joint Computer Conference, pp. 281–285 (1970)
3. Okada, H., Igarashi, Y., Nakanishi, Y.: Analysis and application of framed ALOHA channel in satellite packet switching networks - FADRA method. Electron. Commun. Japan **60**, 72–80 (1977)
4. Choudhury, G., Rappaport, S.: Diversity ALOHA - a random access scheme for satellite communications. IEEE Trans. Commun. **31**(3), 450–457 (1983)
5. Casini, E., De Gaudenzi, R., Del Rio Herrero, O.: Contention resolution diversity slotted ALOHA (CRDSA): an enhanced random access schemefor satellite access packet networks. IEEE Trans. Wirel. Commun. **6**(4), 1408–1419 (2007)
6. Liva, G.: Graph-based analysis and optimization of contention resolution diversity slotted ALOHA. IEEE Trans. Commun. **59**(2), 477–487 (2011)
7. Paolini, E., Liva, G., Chiani, M.: Coded slotted ALOHA: a graph-based method for uncoordinated multiple access. IEEE Trans. Inf. Theory **61**(12), 6815–6832 (2015)
8. Zorzi, M., Rao, R.R.: Capture and retransmission control in mobile radio. IEEE J. Sel. Areas Commun. **12**(8), 1289–1298 (1994)
9. Ren, W., Ward, J., Hodgart, S., Sweeting, M.: Modelling of capture effect and analysis in LEO satellite channel. In: 2000 IEEE International Conference on Communications, ICC 2000, vol. 1, pp. 124–128 (2000)
10. Corazza, G.E., Vatalaro, F.: A statistical model for land mobile satellite channels and its application to nongeostationary orbit systems. IEEE Trans. Veh. Technol. **43**(3), 738–742 (1994)
11. Richardson, T., Urbanke, R.: Modern Coding Theory. Cambridge University Press, Cambridge (2008)